Performance Analysis of Orthogonal-Code Hopping Multiplexing Systems With Repetition, Convolutional, and Turbo Coding Schemes

Bang Chul Jung, *Student Member, IEEE*, and Dan Keun Sung, *Senior Member, IEEE*

***Abstract*—In orthogonal-code hopping multiplexing (OCHM) systems, hopping-pattern (HP) collisions may degrade system performance. Previous studies on the effect of HP collisions in OCHM systems were based on computer simulations, and there was no mathematical analysis of the bit-error-rate (BER) performance. The HP collisions in OCHM systems differ from hits in frequency-hopping systems or intracell interference in direct-sequence code-division multiple-access (DS/CDMA) systems because they can effectively be controlled through synergy and perforation techniques. In this paper, we introduce a received-signal model for OCHM systems called a perforation-only model and analyze the BER performance for OCHM systems in both uncoded and coded environments. Repetition, convolutional, and turbo codes are considered in coded environments. Through the analysis of BER performance, OCHM systems can more clearly be characterized, and the allocated power at the base station (BS) can be estimated for OCHM systems. Furthermore, the user capacity is analyzed for a given channel coding scheme. The results show that the uncoded BER is saturated by the perforation probability, and the coded BER is degraded as the perforation probability increases. We investigate the allocated power at the BS according to the perforation probability and compare the user capacities of OCHM systems using the three different types of coding schemes.**

***Index Terms*—Bit-error-rate (BER) analysis, convolutional codes (CCs), orthogonal-code hopping multiplexing (OCHM), power allocation, repetition codes (RCs), turbo codes (TCs), user capacity.**

I. Introduction

RECENTLY, data traffic has gradually increased in wireless communication systems, and it is expected to be dominant in future wireless systems. Data traffic is inherently bursty and generally exhibits low user activities. Furthermore, there is more downlink traffic than uplink traffic. Several efficient downlink systems have been proposed to provide this data traffic in wireless link [1], [2].

An orthogonal-code hopping multiplexing (OCHM) system [3]–[7] has been proposed to accommodate a larger number of mobile users (MUs) with bursty traffic than the number of orthogonal codewords (OCs) in the downlink. It utilizes statistical multiplexing for orthogonal downlink in direct-sequence code-division multiple-access (DS/CDMA) systems. Since each MU communicates with a base station (BS) through a given orthogonal-code hopping pattern (HP), signaling messages for allocation and deallocation of OCs are not needed during a session. HP can randomly be generated based on an MU-specific number, such as an electronic serial number, and HP collisions between MUs may occur.

When an HP collision among MUs occurs in the conventional frequency-hopping CDMA systems, it is considered to be an inevitable interference (hit) in the case where all MUs are asynchronous with one another [8]. However, the HP collision can be detected and controlled by the BS in a synchronous downlink environment. If HP collisions occur in OCHM systems, the BS compares the user data experiencing an HP collision and determines whether all user data with the same HP collisions are identical or not. If all the corresponding data are identical, the collision does not need to be controlled, and all the colliding symbols of different users are transmitted with a sum of all symbol energies, which results in an energy gain at the receiver. This effect is called synergy. On the contrary, if all data with the same HP collisions are not the same, all the corresponding data symbols are not transmitted (perforation) during the symbol time. Thus, in OCHM systems, the HP collisions do not cause intracell interference (ICI), but they result in information losses. However, they can be recovered by proper channel-coding techniques with additional energy. Therefore, HP collisions in OCHM systems also differ from the ICI, which is characterized by the cross-correlation function between non-OCs, in the uplink of DS-CDMA systems.

Previous studies [3]–[7] on the OCHM systems have focused on the mitigation of the perforation effect. However, the performance of these proposed schemes was mainly evaluated based on computer simulations, particularly in terms of the frame-error rate (FER) for given perforation probabilities and received E_b/N_0 values. Thus far, there has been no rigorous mathematical analysis for the effect of perforations on the system performance. In this paper, we introduce a received-signal model for OCHM systems and analyze the BER performance in both uncoded and coded environments. Based on the BER performance, the FER performance at the MU can be estimated, and the user capacity of the OCHM system is also analyzed for a given channel coding scheme. Furthermore, the allocated power for each MU at the BS can be estimated.

The rest of this paper is organized as follows. In Section II, a received-signal model for OCHM systems is introduced.

Manuscript received August 21, 2006; revised February 23, 2007 and May 29, 2007. This work was supported in part by the BroMA IT Research Center Project. The review of this paper was coordinated by Dr. A. Chockalingam.

The authors are with the Department of Electrical Engineering and Computer Science, Korea Advanced Institute of Science and Technology, Daejeon 305 701, Korea (e-mail: bcjung@cnr.kaist.ac.kr; dksung@ee.kaist.ac.kr).

Digital Object Identifier 10.1109/TVT.2007.905598

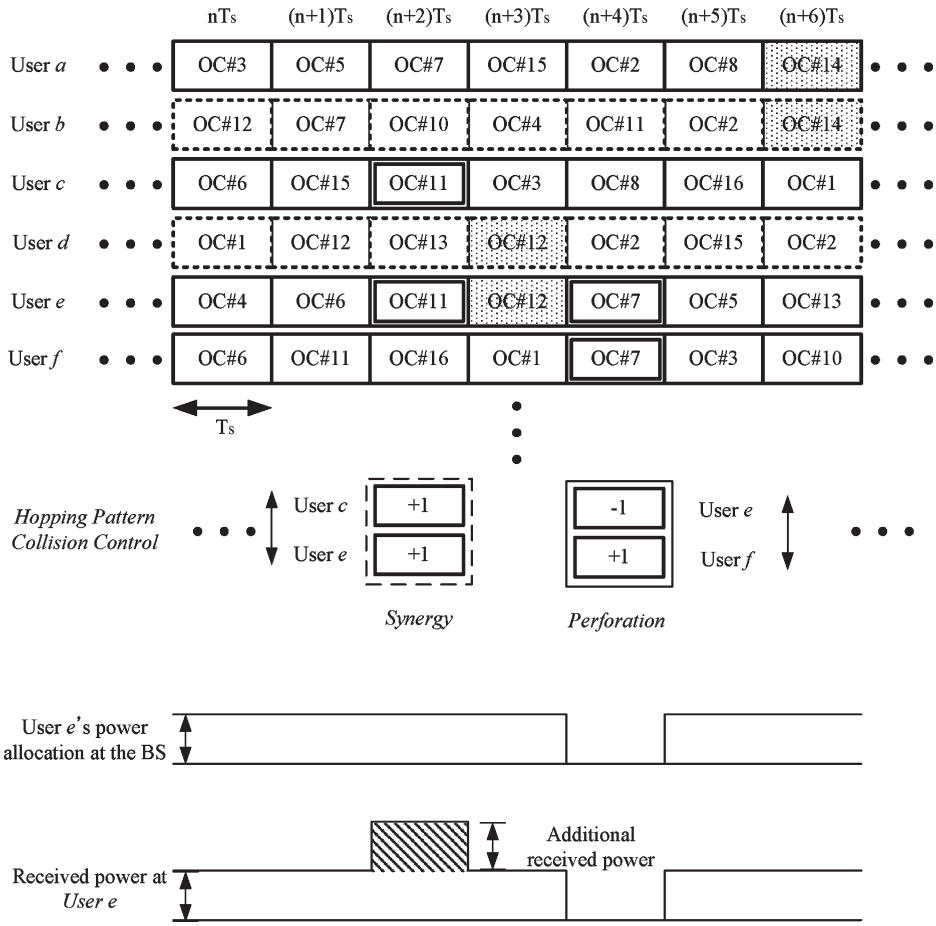

Fig. 1. Block diagram of the OCHM system.

In Section III, the BER performance of OCHM systems is analyzed in both uncoded and coded environments when the perforation is only considered at the receiver. The performance of OCHM systems is analyzed in terms of the required power at BS and user capacity in Section IV. Numerical examples for the performance are shown in Section V. Finally, conclusions are presented in Section VI.

II. Received-Signal Model in OCHM Systems

A. OCHM Mechanism, HP Collisions, Perforation, and Synergy

OCHM systems utilize a synergy and perforation scheme for HP-collision control at the BS. Fig. 1 shows the block diagram of an OCHM system deploying the synergy and perforation scheme. Furthermore, both the transmitted- and received-power levels for a specific user are shown. $T_{\rm s}$ denotes the symbol time. Each user changes the OC according to the HP at each symbol time, during which an HP collision may occur. However, most of users may be inactive because of low channel activities when they demand data services. Users b and d are inactive in Fig. 1, but they follow their HPs during their sessions. In this case, HP collisions between an active user group and an inactive user group do not affect the performance of the active user group. The shaded parts in Fig. 1 indicate this type of collision.

When an HP collision among the active users occurs, a BS compares the user data experiencing the HP collision and determines whether all user data with the same HP collision are the same or not. If all the corresponding data are the same, all the corresponding data symbols are transmitted (synergy) without control, which results in an energy gain at the receiver. On the contrary, if all data with the same HP collisions are not the same, all the corresponding data symbols are not transmitted (perforated) during the symbol time. For example, user e experiences a synergy at $(n+2)T_{\rm s}$ and a perforation at $(n+4)T_{\rm s}$.

When a user experiences a synergy, BS allocates power for the user without any change, and then, all the symbols experiencing the synergy have an additional energy at the receivers because of other users' energy added by despreading process using the same OC. The quantity of the additional power is determined by the distance between a BS and users with code collisions in case that the OCHM system utilizes a power-control scheme. In Fig. 1, if user e is at a cell boundary and user c is located near a BS, the additional received power at user e is much smaller than the original received power, which is the power when an HP collision does not occur. On the contrary, the additional received power at user c is much bigger than the original received power in case of an HP collision. The synergy scheme results in an energy gain. However, its effect varies according to the location of users in a cell. Statistically, the users near a BS have a larger energy gain than those at the

cell boundary. Therefore, in OCHM systems, the energy gain at the receiver due to the synergy scheme is complex to analyze even though several previous papers assumed that all the HP-collision users are located in the same distance from a BS in their performance evaluations [3]–[7].

When a user experiences a perforation, BS does not allocate power for the perforated symbol, and the user detects only noise during the perforated symbol time. Hence, the perforation degrades the BER performance, and the additional energy may be required to meet for a target BER.

The HP-collision probability of the OCHM system is expressed as

$$P_{\mathrm{c}} = 1 - \left(1 - \frac{\bar{v}}{N_{\mathrm{OC}}}\right)^{M-1} \tag{1}$$

where $\bar{v}$ is the channel activity, N_{OC} is the number of OCs, and M is the number of active users in a cell. For a given channel activity $\bar{v}$, P_{c} increases as the number of active users increases. The perforation probability of encoded symbols in the conventional OCHM systems is written as

$$P_{\mathrm{p}} = 1 - \left(1 - \frac{m-1}{m} \cdot \frac{\bar{v}}{N_{\mathrm{OC}}}\right)^{M-1} \tag{2}$$

where m is the number of symbol locations in data modulation [i.e., $m = 2$ for binary phase shift keying (BPSK)]. Hence, the synergy probability is given as

$$P_{\mathrm{s}} = P_{\mathrm{c}} - P_{\mathrm{p}}. \tag{3}$$

B. Perforation-Only Model (POM)

In this model, we assume that the additional received power is set to zero. Hence, this signal model provides a lower bound of the BER performance of OCHM systems. The received-signal model of the BPSK symbol in additive white Gaussian noise (AWGN) channel is expressed as

$$Y = \begin{cases} t_1 \sim N(0, \sigma^2), & \text{if perforation} \\ t_2 \sim N\left(\sqrt{E_{\mathrm{s}}}, \sigma^2\right), & \text{otherwise.} \end{cases} \tag{4}$$

$x \sim N(\mu, \sigma^2)$ represents that x is a Gaussian random variable with mean μ and variance σ^2. In (4), we also assume that a positive symbol is transmitted, and its symbol energy is E_{s}. We call this model a POM because it considers the perforation effect when HP collisions occur. The distribution function of POM is obtained as

$$F_Y(y) = G\left(\frac{y}{\sigma}\right) \cdot P_{\mathrm{p}} + G\left(\frac{y - \sqrt{E_{\mathrm{s}}}}{\sigma}\right) \cdot (1 - P_{\mathrm{p}}) \tag{5}$$

where

$$G\left(\frac{x-\mu}{\sigma}\right) = \int_{-\infty}^{x} \frac{1}{\sqrt{2\pi\sigma^2}} e^{-(x-\mu)^2/2\sigma^2} dx.$$

Therefore, the probability density function (pdf) of the received signal in OCHM systems is given as

$$f_Y(y) = P_{\mathrm{p}} \cdot \frac{1}{\sqrt{2\pi\sigma^2}} e^{-y^2/2\sigma^2} + (1 - P_{\mathrm{p}}) \cdot \frac{1}{\sqrt{2\pi\sigma^2}} e^{-\left(y - \sqrt{E_{\mathrm{s}}}\right)^2/2\sigma^2} \tag{6}$$

where the received signal follows the POM. As noted earlier, the POM provides the upper bound of the BER performance of OCHM systems. Furthermore, POM maintains the consistency regardless of the distance between the MU and the BS, since the perforation effect is not dependent on the relative distance. The BER performance in POM provides the overall system performance regardless of the MU's location for a given perforation probability. Therefore, we utilize POM for the BER performance analysis in the rest of this paper.

III. BER Performance Analysis in POM

A. Uncoded BER Performance

In (4), we assume that the positive symbol is transmitted with a symbol energy of E_{s}. In an AWGN channel, a bit error occurs when the received symbol has a negative phase. Therefore, the bit-error probability in POM is given as

$$\begin{aligned} P_{\mathrm{b,uncoded}}^{\mathrm{OCHM}} &= P\{Y \le 0\} \\ &= G(0) \cdot P_{\mathrm{p}} + G\left(\frac{-\sqrt{E_{\mathrm{s}}}}{\sigma}\right) \cdot (1 - P_{\mathrm{p}}) \\ &= \frac{P_{\mathrm{p}}}{2} + (1 - P_{\mathrm{p}}) \cdot Q\left(\sqrt{\frac{2E_{\mathrm{s}}}{N_0}}\right) \\ &= \frac{P_{\mathrm{p}}}{2} + (1 - P_{\mathrm{p}}) \cdot Q\left(\sqrt{\frac{2E_b}{N_0 \cdot (1 - P_{\mathrm{p}})}}\right). \end{aligned} \tag{7}$$

Note that the symbol energy of the OCHM systems is not equal to the bit energy even when the system is assumed to be in an uncoded environment. For comparison with the conventional BPSK scheme, the energy for the perforated symbol is assumed to be utilized for the other symbols. The second term in (7) becomes zero as the signal-to-noise ratio increases, but the first term is residual. Therefore, the uncoded bit-error probability of the OCHM systems is saturated by the perforation probability.

B. Coded BER Performance of Repetition Codes (RCs)

RC is simply to repeat the information n-times and, thus, the code rate becomes $1/n$. If we use a soft-decision decoder at the receiver, RC has no coding gain, as compared with the uncoded systems in AWGN. However, as proposed in [9], the repetition can be effective to mitigate the perforation effect and reduce the additional required E_b/N_0 in OCHM systems. First, we consider the BER performance of an RC in the conventional system where there are no HP collisions. In a binary RC, there are only two codewords, such as $\mathbf{S}_0 = \{0, 0, \ldots, 0\}$, if the information $(\mathbf{b})$ is zero and $\mathbf{S}_1 = \{1, 1, \ldots, 1\}$ if the information $(\mathbf{b})$ is one. If the received-signal vector is given as $\mathbf{y} = \{y_1, y_2, \ldots, y_n\}$, the maximum-likelihood decoder compares the likelihood of

each codeword for a given received vector. Hence, the log-likelihood ratio (LLR) of the information bit is given by

$$\Lambda(\mathbf{b}) = \ln \frac{P\{\mathbf{y}|\mathbf{S}_1\}}{P\{\mathbf{y}|\mathbf{S}_0\}}. \tag{8}$$

We consider a BPSK modulation, with coded bits in the set $\{0, 1\}$ mapped onto real values $\{-\sqrt{E_\mathrm{s}}, +\sqrt{E_\mathrm{s}}\}$, respectively, and each received symbol in the received vector is assumed to statistically be independently and identically distributed. Then, (8) is written as

$$\begin{aligned}\Lambda(\mathbf{b}) &= \ln \frac{\exp\left\{-\frac{\left(y_1-\sqrt{E_\mathrm{s}}\right)^2}{2\sigma^2}\right\}\cdots\exp\left\{-\frac{\left(y_n-\sqrt{E_\mathrm{s}}\right)^2}{2\sigma^2}\right\}}{\exp\left\{-\frac{\left(y_1+\sqrt{E_\mathrm{s}}\right)^2}{2\sigma^2}\right\}\cdots\exp\left\{-\frac{\left(y_n+\sqrt{E_\mathrm{s}}\right)^2}{2\sigma^2}\right\}} \\ &= \sum_{i=1}^{n}\frac{2\sqrt{E_\mathrm{s}}}{\sigma^2}y_i. \end{aligned}\tag{9}$$

If the LLR is larger than zero, the decoded bit becomes one, and otherwise, the decoded bit becomes zero. Hence, the bit-error probability is given as

$$P_\mathrm{b}^{\mathrm{RC}} = P\left\{\Lambda(\mathbf{b}) < 0|\mathbf{S}_1 \text{ is transmitted}\right\} = P\{Z < 0\}$$

where

$$Z = \sum_{r=i}^{n} y_i. \tag{10}$$

Z is the sum of n independent Gaussian random variables, each with mean $+\sqrt{E_\mathrm{s}}$ and variance $N_0/2$, i.e., Z is a Gaussian random variable with mean $n\sqrt{E_\mathrm{s}}$ and variance $nN_0/2$. Thus, (10) can be written as

$$\begin{aligned}P_\mathrm{b}^{\mathrm{RC}} &= Q\left(\sqrt{\frac{2nE_\mathrm{s}}{N_0}}\right) = Q\left(\sqrt{\frac{2nR_\mathrm{c}E_b}{N_0}}\right) \\ &= Q\left(\sqrt{\frac{2E_b}{N_0}}\right)\end{aligned}\tag{11}$$

where R_c indicates the code rate of the encoder and it is equal to $1/n$, since an n-RC is assumed to be used. Note that the BER performance of the RC in the conventional system is equal to that of the uncoded BPSK system. Although the RC has no coding gain in the conventional system, it can be an effective coding scheme in the OCHM system because it decentralizes the perforation effect over the repeated symbols, and the full-perforation probability in which all repeated symbols are perforated is reduced.

We now consider the OCHM system with a POM. In OCHM systems, the bit-error probability is obtained by substituting (6) for the pdf of y_i into (10). This method is also useful for analyzing the BER performance of the convolutional codes (CCs).

We use the characteristic function of a random variable for analysis. The characteristic function of a Gaussian random variable $N(\mu, \sigma^2)$ is given as [10]

$$\Phi_X(w) = \exp\left\{j\mu w - \frac{1}{2}\sigma^2 w^2\right\}. \tag{12}$$

When we consider the POM case in OCHM systems, the characteristic function of the received signal in OCHM systems is obtained by

$$\begin{aligned}\Phi_Y(w) = P_\mathrm{p}\cdot\exp\left\{-\frac{1}{2}\sigma^2 w^2\right\} \\ + (1-P_\mathrm{p})\cdot\exp\left\{j\sqrt{E_\mathrm{s}}w - \frac{1}{2}\sigma^2 w^2\right\}.\end{aligned}\tag{13}$$

Then, the characteristic function of the random variable Z is expressed as

$$\Phi_Z(w) = \Phi_{Y_1}(w)\Phi_{Y_2}(w), \ldots, \Phi_{Y_n}(w) = [\Phi_Y(w)]^n \tag{14}$$

where each received signal y_i in OCHM systems has the same pdf and is independent of each other. Substituting (13) into (14) yields the characteristic function of Z as follows:

$$\Phi_Z(w) = \sum_{i=0}^{n}\binom{n}{i}(1-P_\mathrm{p})^i P_\mathrm{p}^{n-i} e^{jw\sqrt{E_\mathrm{s}}\cdot i - \frac{\sigma^2 w^2 n}{2}}. \tag{15}$$

Therefore, the probability density and distribution functions of Z are obtained as

$$f_Z(z) = \sum_{i=0}^{n}\binom{n}{i}(1-P_\mathrm{p})^i P_\mathrm{p}^{n-i}\frac{1}{2\pi n\sigma^2}e^{\frac{-(z-i\sqrt{E_\mathrm{s}})^2}{2n\sigma^2}} \tag{16}$$

and

$$F_Z(z) = \sum_{i=0}^{n}\binom{n}{i}(1-P_\mathrm{p})^i P_\mathrm{p}^{n-i}\cdot G\left(\frac{z-i\sqrt{E_\mathrm{s}}}{\sqrt{n}\sigma}\right). \tag{17}$$

From (17), the bit-error probability of the n-RC in OCHM systems is expressed as

$$P_{\mathrm{b,RC}}^{\mathrm{OCHM}} = \sum_{i=0}^{n}\binom{n}{i}(1-P_\mathrm{p})^i P_\mathrm{p}^{n-i} Q\left(\sqrt{\frac{2i^2E_b}{nN_0(1-P_\mathrm{p})}}\right) \tag{18}$$

where i represents the number of nonperforated symbols among n repeated symbols. Hence, $i = 0$ indicates that all symbols in n-times repeated symbols are perforated. In (18), the bit-error

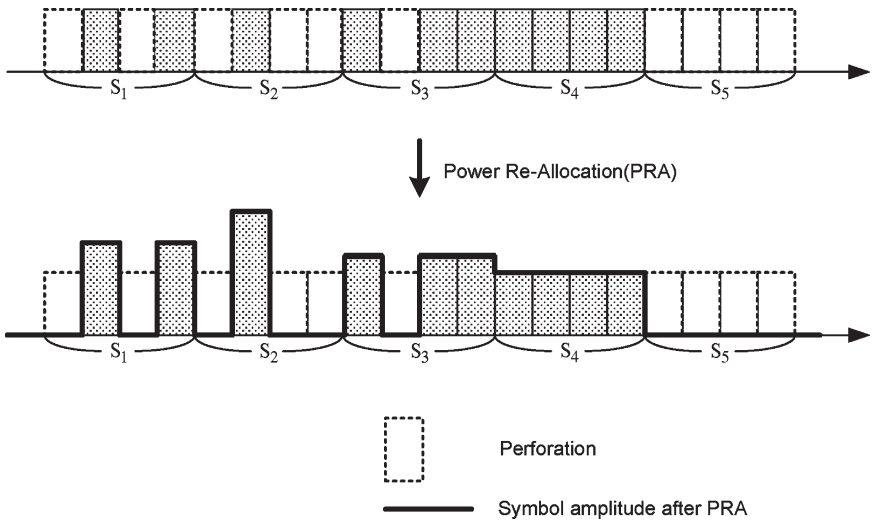

Fig. 2. Block diagram of an RC with power-reallocation technique.

probability can be divided into the following two cases: $i = 0$ and $i \neq 0$. Equation (18) is rewritten as

$$P_{\mathrm{b,RC}}^{\mathrm{OCHM}} = \sum_{i=1}^{n} \binom{n}{i} (1-P_{\mathrm{p}})^i P_{\mathrm{p}}^{n-i} \cdot Q\left(\sqrt{\frac{2i^2 E_b}{nN_0(1-P_{\mathrm{p}})}}\right) + \frac{(P_{\mathrm{p}})^n}{2} \quad (19)$$

where the last term indicates the full-perforation situation in the repeated symbols. As the E_b/N_0 value increases, the first term in the right-hand side of (19) becomes zero, but the last term in (19) is residual. Hence, the bit-error probability of the RC in OCHM system becomes saturated to $(P_{\mathrm{p}})^n/2$, which is determined by the full-perforation probability $(P_{\mathrm{p}})^n$. Note that the saturated bit-error probability of an RC is smaller than that of the uncoded system, as shown in (7). Therefore, the RC is an effective coding scheme in OCHM systems, although it has no benefit in the conventional system in terms of BER.

C. Coded BER Performance of RCs With Power-Reallocation Technique

We proposed a symbol repetition-and-power-reallocation (PRA) scheme in reducing the perforation effect in OCHM systems, but we have not analyzed the BER performance of the proposed scheme [9]. We propose an RC with PRA (RC-PRA) scheme and analyze its performance in this paper. Fig. 2 shows the block diagram of the proposed RC-PRA in OCHM systems. Each symbol is repeated four times, and some of the repeated symbols may be perforated. The number of perforations in symbols 1, 2, and 3 is two, three, and one, respectively. Symbol 4 has no perforations, and the repeated symbols of Symbol 5 are all perforated. We define a partial perforation in which there exist $j(0 < j < n)$ perforations among n-repeated symbols (e.g., Symbols 1–3) and a full perforation in which all repeated symbols are perforated (e.g., Symbol 5). If a symbol experiences a partial perforation, the remaining symbols are used for decoding the original symbol. However, if a symbol suffers from a full perforation, the original symbol cannot be recovered, and it causes a BER performance saturation as noted earlier. Note that the power allocated to Symbol 1 is different from that of Symbol 2. Since two symbols have a different number of perforated symbols, the number of the remaining symbols is also different. We propose to adjust the power level of the remaining symbols to maintain the same energy regardless of the number of perforations unless the symbol experiences a full perforation. Through this process, we can receive all symbols with the same energy unless the symbol experiences a full perforation. If the symbol experiences a full perforation, its energy is utilized for the other symbols for comparison with the conventional systems.

The received signal of the proposed n-times RC-PRA system is expressed as

$$Y = \begin{cases} t_1 \sim N(0, \sigma^2), & \text{if full perforation} \\ t_2 \sim N\left(\sqrt{\frac{n}{n-j}E_{\mathrm{s}}}, \sigma^2\right), & \text{otherwise} \end{cases} \quad (20)$$

where j represents the number of perforations among n-repeated symbols $(0 \leq j < n)$. The pdf of the received signal for a given j in the POM is written as

$$f_Y(y|j) = \frac{j}{n} \cdot \frac{1}{\sqrt{2\pi\sigma^2}} e^{-y^2/2\sigma^2} + \frac{n-j}{n} \cdot \frac{1}{\sqrt{2\pi\sigma^2}} e^{-\left(y-\sqrt{\frac{n}{n-j}E_{\mathrm{s}}}\right)^2/2\sigma^2} \quad (21)$$

where the transmitted information is assumed to be one according to the used mapping rule in Section III-B. Hence, the decision statistic for a given j is expressed as

$$Z_j \sim N\left(\sqrt{n(n-j)E_{\mathrm{s}}}, n\sigma^2\right) \quad (22)$$

since $Z_j = j \cdot t_1 + (n-j) \cdot t_2$, where t_1 and t_2 are defined in (20). The pdf of Z_j is given as

$$F_{Z_j} = G\left(\frac{y - \sqrt{n(n-j)E_{\rm s}}}{\sqrt{n}\sigma}\right). \tag{23}$$

The bit-error probability of the proposed RC-PRA scheme is given as

$$\begin{aligned}\tilde{P}_{\rm b,RC}^{\rm OCHM} &= P(z \le 0) \\ &= \sum_{j=0}^{n} P(j \text{ perforations} \mid n \text{ repetitions}) \cdot F_{Z_j}(0) \\ &= \sum_{j=0}^{n} \binom{n}{j} (1-P_{\rm p})^{n-j} P_{\rm p}^{j} \cdot G\left(\frac{y-\sqrt{n(n-j)E_{\rm s}}}{\sqrt{n}\sigma}\right) \\ &= \sum_{i=0}^{n} \binom{n}{i} (1-P_{\rm p})^{i} P_{\rm p}^{n-i} \cdot Q\left(\sqrt{\frac{2iE_b}{nN_0\,(1-(P_{\rm p})^n)}}\right)\end{aligned} \tag{24}$$

where $i = n - j$, and the code rate is $1/n$. Note that $E_{\rm s} = E_b/[n(1-(P_{\rm p})^n)]$ in (24), since only the energy for a full perforated symbol is utilized for other symbols in the proposed scheme. The proposed RC-PRA has the same saturated bit-error probability for $i = 0$ in (24), as that of the conventional RC in the OCHM systems. However, the proposed RC-PRA has the improved bit-error performance as compared with the conventional RC. We will compare the performance between the two schemes in Section V.

D. Coded BER Performance of CCs

We now consider the coded bit-error probability of the OCHM systems with the CCs. CC is one of the most commonly used channel coding schemes in wireless communication systems. We assume that BPSK modulation is used for transmitted coded symbols over an AWGN channel with one-sided power-spectral density N_0. For the soft-decision Viterbi decoder, the probability of error in the pairwise comparison of two paths at a node that differ in d symbols is expressed as [12]

$$P_d = P\left\{\sum_{r=1}^{d} y_r \le 0\right\} \tag{25}$$

where y_r represents the rth received symbol. Equation (25) is called the first-event-error probability. When we assume that an all-zero codeword is transmitted according to the mapping $0 \to +\sqrt{E_{\rm s}}$, $Z = \sum_{r=1}^{d} y_r$ is the sum of d independent Gaussian random variables, each with mean $\sqrt{E_{\rm s}}$ and variance $N_0/2$, i.e., Z is a Gaussian random variable with mean $d\sqrt{E_{\rm s}}$ and variance $dN_0/2$. This is very similar to the case of RC. Thus, (25) can be written as

$$P_d = Q\left(\sqrt{\frac{2dE_{\rm s}}{N_0}}\right) = Q\left(\sqrt{\frac{2dR_{\rm c}E_b}{N_0}}\right) \tag{26}$$

where $R_{\rm c}$ denotes the code rate of the encoder. From (25) and (26), the event- and bit-error probability bounds of CCs in AWGN channels are expressed as [12]

$$P_{\rm e} < \sum_{d=d_{\rm free}}^{\infty} A_d Q\left(\sqrt{\frac{2dR_{\rm c}E_b}{N_0}}\right) \tag{27}$$

$$P_{\rm b} < \sum_{d=d_{\rm free}}^{\infty} B_d Q\left(\sqrt{\frac{2dR_{\rm c}E_b}{N_0}}\right) \tag{28}$$

where A_d and B_d are the number of codewords of weight d, and the total number of nonzero information bits on all weight d codewords, respectively [13]. $d_{\rm free}$ is the free distance of CCs.

Using (13)–(17), the first-event-error probability of the CCs in OCHM systems is expressed as

$$P_{d,\rm CC}^{\rm OCHM} = \sum_{i=0}^{d} \binom{d}{i} (1-P_{\rm p})^{i} P_{\rm p}^{d-i} \cdot Q\left(\sqrt{\frac{2i^2R_{\rm c}E_b}{dN_0(1-P_{\rm p})}}\right). \tag{29}$$

Hence, the event- and bit-error probability bounds in OCHM systems with the CCs are expressed as

$$P_{\rm e,CC}^{\rm OCHM} < \sum_{d=d_{\rm free}}^{\infty} A_d \sum_{i=0}^{d} \binom{d}{i} (1-P_{\rm p})^{i} P_{\rm p}^{d-i} \cdot Q\left(\sqrt{\frac{2i^2R_{\rm c}E_b}{dN_0(1-P_{\rm p})}}\right) \tag{30}$$

and

$$P_{\rm b,CC}^{\rm OCHM} < \sum_{d=d_{\rm free}}^{\infty} B_d \sum_{i=0}^{d} \binom{d}{i} (1-P_{\rm p})^{i} P_{\rm p}^{d-i} \cdot Q\left(\sqrt{\frac{2i^2R_{\rm c}E_b}{dN_0(1-P_{\rm p})}}\right) \tag{31}$$

where A_d and B_d are determined by the encoder structure. Using the bound $Q(x) < \exp(-x^2/2)$, we obtain the expression

$$P_{\rm b,CC}^{\rm OCHM} < \sum_{d=d_{\rm free}}^{\infty} B_d \sum_{i=0}^{d} \binom{d}{i} (1-P_{\rm p})^{i} P_{\rm p}^{d-i} \cdot \exp\left(\frac{-i^2R_{\rm c}E_b}{dN_0(1-P_{\rm p})}\right). \tag{32}$$

Furthermore, for large values of E_b/N_0, the first term in the bit weight-enumerating function (WEF) dominates the bound of (32), we can approximate $P_{\rm b,CC}^{\rm OCHM}$ as

$$P_{\rm b,CC}^{\rm OCHM} \approx B_{d_{\rm free}} \sum_{i=0}^{d_{\rm free}} \binom{d_{\rm free}}{i} (1-P_{\rm p})^{i} P_{\rm p}^{d_{\rm free}-i} \cdot \exp\left(\frac{-i^2R_{\rm c}E_b}{d_{\rm free}N_0(1-P_{\rm p})}\right). \tag{33}$$

The CC also has the saturated bit-error probability in OCHM systems. For large values of E_b/N_0, the bit-error probability from the free distance in the WEF dominates the overall bit-error probability. Hence, we can approximate the BER

performance as the case of $d = d_{\text{free}}$ in (31). The bit-error probability of the CC is saturated to

$$\frac{B_{\text{free}}(P_{\text{p}})^{d_{\text{free}}}}{2}. \tag{34}$$

E. Coded BER Performance of Turbo Codes (TCs)

The original concept of TCs was introduced in [15], and for the first time, the theoretical justification for the performance of TC was provided by Benedetto and Montorsi in [16], [17]. A TC yields excellent performance that is very close to the Shannon limit at low and medium E_b/N_0 values. However, the TC-performance curve shows a slope change at high E_b/N_0 values if the code free distance is small. This phenomenon is called an error floor. In fact, the BER performance of TC at the low or medium E_b/N_0 values is hard to analyze, and most previous works on the TC performance assumed relatively high E_b/N_0 values, which represents an error-floor region. Under this assumption, the bit-error probability of the TCs is expressed as

$$P_{\text{b,TC}} \approx \frac{W_{\text{free}}}{L_{\text{frame}}} \cdot Q\left(\sqrt{\frac{2d_{\text{free}}R_{\text{c}}E_{\text{b}}}{N_0}}\right) \tag{35}$$

where L_{frame} and W_{free} indicate the frame length and the information-bit multiplicity of the free distance, respectively. Equation (35) is based on the fact that the coded performance for high E_b/N_0 values essentially coincides with the union bound truncated to the contribution of the free distance, similar to the CC case. Note that the BER performance of the TC is also determined by the information-block length, which is known as interleaving gain, as well as the free distance and its multiplicity. Furthermore, the interleaver structure is the most important component for good performance in the TC since it determines the free distance and its multiplicity.

We need to compute the first several terms of the distance spectrum in order to produce a more accurate estimate, particularly at the E_b/N_0 values where a slope change occurs. If we now evaluate the expression of the truncated union bound by taking into account the contribution of several terms of its distance spectrum, we obtain the truncated union bound

$$UB(l) \approx \frac{W_{\text{free}}}{L_{\text{frame}}} \cdot Q\left(\sqrt{\frac{2d_{\text{free}}R_{\text{c}}E_{\text{b}}}{N_0}}\right) + \sum_{i=2}^{l} \frac{W_i}{L_{\text{frame}}} \cdot Q\left(\sqrt{\frac{2d_iR_{\text{c}}E_{\text{b}}}{N_0}}\right) \tag{36}$$

where d_i and W_i indicate the ith distance and its bit multiplicity of the distance spectrum, respectively. For concatenated codes, a small penalty (usually less than 0.5 dB) must be also taken into account due to the suboptimality of iterative decoding [18]. Through (35) and (36), the bit-error probability at high E_b/N_0 values is estimated, and its slope is obtained. In most cases, d_i and W_i are not easy to find since they are related to the interleaver structure. There have been many studies on the calculation of the free distance and its multiplicity of the TCs for a given interleaver [18], [19]. In this paper, we compute the distance spectrum coefficients according to the method in [19].

TABLE I
SATURATED BER COMPARISON OF VARIOUS CODING SCHEMES

Uncoded	RC	RC-PRA	CC	TC
$\frac{P_p}{2}$	$\frac{(P_p)^n}{2}$	$\frac{(P_p)^n}{2}$	$\frac{B_{free}(P_p)^{d_{free}}}{2}$	$\frac{W_{free}(P_p)^{d_{free}}}{2L_{frame}}$

When TC is used for OCHM systems, we can approximate the bit-error probability using error-floor analysis [(35)] or truncated-union-bound analysis [(36)]. Basically, the bit-error-probability analysis of a TC is similar to that of the CC cases, except for the computation of distance spectrum coefficients. From the previous analysis of the CC, the bit-error probability of the TC is expressed as

$$P_{\text{b,TC}}^{\text{OCHM}} \approx \frac{W_{\text{free}}}{L_{\text{frame}}} \cdot \sum_{i=0}^{d_{\text{free}}} \binom{d_{\text{free}}}{i} (1-P_{\text{p}})^i P_{\text{p}}^{d_{\text{free}}-i} \cdot Q\left(\sqrt{\frac{2i^2R_{\text{c}}E_{\text{b}}}{d_{\text{free}}N_0(1-P_{\text{p}})}}\right) \tag{37}$$

and

$$UB^{\text{OCHM}}(l) \approx \sum_{j=1}^{l} \frac{W_j}{L_{\text{frame}}} \cdot \sum_{i=0}^{d_j} \binom{d_j}{i} (1-P_{\text{p}})^i P_{\text{p}}^{d_j-i} \cdot Q\left(\sqrt{\frac{2i^2R_{\text{c}}E_{\text{b}}}{d_jN_0(1-P_{\text{p}})}}\right) \tag{38}$$

where $d_1 = d_{\text{free}}$, and $W_1 = W_{\text{free}}$, respectively. In addition, the saturated bit-error probability of a TC in OCHM systems is obtained as

$$\frac{W_{\text{free}}(P_{\text{p}})^{d_{\text{free}}}}{2L_{\text{frame}}}. \tag{39}$$

F. BER-Saturation Comparison

As we noted in the previous sections, both uncoded and coded schemes have the BER saturation. The saturated BER is important since it can limit the user capacity. If the saturated BER for a given P_{p} values is larger than the required BER for a specific service, the OCHM system cannot satisfy the quality of services (QoS) of users. The saturated BER determines the maximum allowable P_{p} value for the specific coding scheme, which is derived from the number of users, and thus, the saturated BER limits the maximum number of users in a cell when the user capacity is limited only by the number of codes. Table I summarizes the saturated BER of the three different coding schemes.

IV. PERFORMANCE ANALYSIS FOR OCHM SYSTEMS

A. FER Analysis From the BER Performance Analysis

In data communications, FER is important because even a single bit error in a frame may make the frame useless. Thus,

most mobile communication systems choose the FER as a QoS parameter. A reasonable approximation for FER of a channel coding scheme is given by

$$\begin{aligned}\mathrm{FER} &\simeq 1-(1-P_{\mathrm{b}})^{L_{\mathrm{frame}}}\\ &\simeq P_{\mathrm{b}}\cdot L_{\mathrm{frame}}\end{aligned} \tag{40}$$

where $P_{\mathrm{b}}(P_{\mathrm{b}} \ll 1)$ and L_{frame} denote the bit-error probability of a channel coding scheme and the frame length, respectively. This approximation is also valid for a TC. The FER of a TC can be expressed as [19]

$$\begin{aligned}\mathrm{FER}_{\mathrm{TC}} &\approx W_{\mathrm{free}}\cdot Q\left(\sqrt{\frac{2d_{\mathrm{free}}R_{\mathrm{c}}E_{\mathrm{b}}}{N_0}}\right)\\ &= L_{\mathrm{frame}}\cdot P_{\mathrm{b,TC}}.\end{aligned} \tag{41}$$

For a given P_{p} value, if $\mathrm{FER}_{\mathrm{req}} < L_{\mathrm{frame}}\cdot P_{\mathrm{b}}^{\mathrm{sat}}$, where $\mathrm{FER}_{\mathrm{req}}$ and $P_{\mathrm{b}}^{\mathrm{sat}}$ indicate the required FER for a specific service and the saturated BER of a specific coding scheme, respectively, the coding scheme cannot be used for the service because a receiver with the coding scheme cannot compensate for the effect of perforations even when the BS transmits the frame with the infinite power.

B. Downlink Power Allocation

In OCHM systems, the downlink power which is allocated for a specific MU is determined by the perforation probability P_{p}, as well as the channel environment. The perforation probability varies according to the number of users in a cell and the user activity at the specific time. Previous work only considered the mean perforation probability according to the number of MUs in a cell. However, the perforation probability of each MU is different from each other. Some MUs have lower or higher perforation probabilities than others at the specific time. In downlink, a BS can know the exact number of perforated symbols in a frame of each MU at the time. Through the BER performance analysis shown in Section III, a BS can determine the allocated power for a specific MU in downlink. If the BER or FER performance analysis does not exist, the link-level simulation results are required in each case.

The additional required E_b/N_0 at an MU due to the perforation can be expressed as

$$\Delta(E_b/N_0) = f(\mathrm{FER}_{\mathrm{req}}, P_{\mathrm{p}}) - f(\mathrm{FER}_{\mathrm{req}}, 0) \tag{42}$$

where $f(A,B)$ denotes the function of the required E_b/N_0 at an MU for $\mathrm{FER}_{\mathrm{req}} = A$ and $P_{\mathrm{p}} = B$, and it is derived from (31) and (40). The last term in (42) indicates the required E_b/N_0 for $P_{\mathrm{p}} = 0$. $\mathrm{FER}_{\mathrm{req}}$ denotes the required FER at receiver. The allocated symbol power for a specific MU at a BS is determined as

$$P_{\mathrm{T}} = \frac{f(\mathrm{FER}_{\mathrm{req}}, P_{\mathrm{p}})\cdot \mu R_{\mathrm{c}}\cdot I_{\mathrm{total}}}{T_{\mathrm{s}}\cdot L_{\mathrm{path}}} \tag{43}$$

where μ, I_{total}, T_{s}, and L_{path} denote the encoded bits per modulated symbol, the total interference at the MU, the symbol time, and the path loss between the BS and the MU, respectively. As P_{p} increases, the required energy at receiver $f(\mathrm{FER}_{\mathrm{req}}, P_{\mathrm{p}})$ increases, and the allocated power P_{T} also increases.

C. User-Capacity Analysis

OCHM was proposed to accommodate more MUs than the number of codewords in downlink of CDMA systems. Recently, we have analyzed the downlink user capacity of OCHM system and have compared it with the user capacity of the conventional CDMA system [6]. In [6], we defined code and power capacities independently like the conventional CDMA systems. Thus, the overall user capacity is derived as the minimum value of two capacities. Code capacity of OCHM systems is defined as the maximum number of HPs for a given P_{p}, which is expressed as

$$M_{\mathrm{c}} = 1 + \frac{\ln(1-P_{\mathrm{p}})}{\ln\left(1-\frac{(m-1)\cdot\bar{\upsilon}}{m\cdot N_{\mathrm{OC}}}\right)}. \tag{44}$$

It is derived from (2). Power capacity is defined as the maximum number of users under the condition that the allocated power is less than or equal to the maximum available power at the BS, and it is expressed as

$$M_{\mathrm{p}} \le \frac{E_{\mathrm{s,max}}\cdot \bar{L}_{\mathrm{path}}}{\bar{\upsilon}\cdot\left(\frac{E_{\mathrm{b}}}{I_0}\right)_{\mathrm{target}}^{\mathrm{OCHM}}\cdot \mu R_{\mathrm{c}}\cdot I_{\mathrm{total}}} \tag{45}$$

where $E_{\mathrm{s,max}}$, $\bar{L}_{\mathrm{path}}$, and $(E_b/I_0)_{\mathrm{target}}^{\mathrm{OCHM}}$ denote the maximum symbol energy for data traffic at the BS, the average path loss at an MU, and the target (E_b/I_0) for a given FER at an MU, respectively. In [6], we have illustrated the user capacity which is the minimum value of (44) and (45) for varying $(E_b/I_0)_{\mathrm{target}}^{\mathrm{OCHM}}$ and P_{p}. $(E_b/I_0)_{\mathrm{target}}^{\mathrm{OCHM}}$ was evaluated through computer simulations for several cases in [6]. However, as we noted in Section IV-B, the additional required energy at an MU increases as P_{p} increases. The allocated power for a specific MU in downlink at a BS also increases as P_{p} increases. Thus, the $(E_b/I_0)_{\mathrm{target}}^{\mathrm{OCHM}}$ value in (45) is dependent on P_{p}. In fact, $(E_b/I_0)_{\mathrm{target}}^{\mathrm{OCHM}} = f(\mathrm{FER}_{\mathrm{req}}, P_{\mathrm{p}})$, and the power capacity of the OCHM system is expressed as

$$\tilde{M}_{\mathrm{p}} \le \frac{E_{\mathrm{s,max}}\cdot \bar{L}_{\mathrm{path}}}{\bar{\upsilon}\cdot f(\mathrm{FER}_{\mathrm{req}}, P_{\mathrm{p}})\cdot \mu R_{\mathrm{c}}\cdot I_{\mathrm{total}}} \tag{46}$$

where $f(\mathrm{FER}_{\mathrm{req}}, P_{\mathrm{p}})$ is determined by the channel-coding capability. We will compare the value of $f(\mathrm{FER}_{\mathrm{req}}, P_{\mathrm{p}})$ and the user capacities of the OCHM system for the three different channel coding schemes in Section V.

V. Numerical Examples

A. BER Performances

A BPSK modulation scheme is used here, and the analysis for BPSK can be used for quadrature phase shift keying. Fig. 3 shows the uncoded BER performance in OCHM systems to vary the perforation probability. The lines represent the

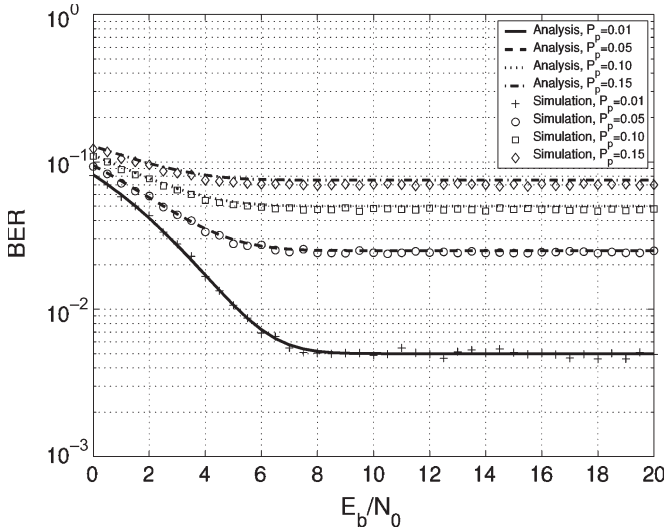

Fig. 3. Uncoded BER performance for varying the perforation probability (P_{p}).

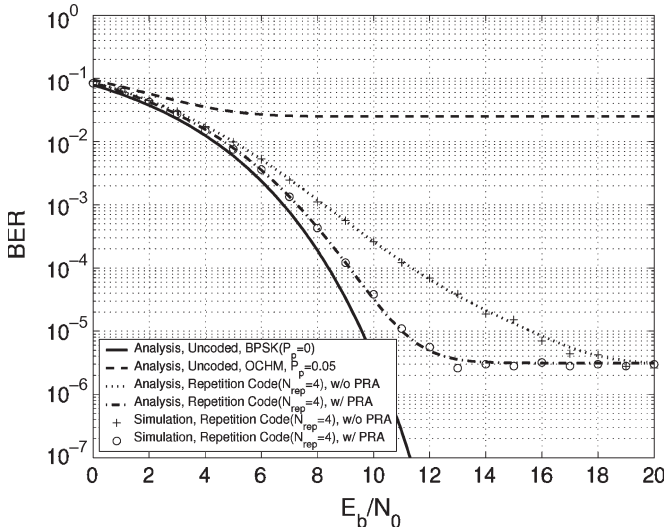

Fig. 4. Coded BER performance of RC with $P_{\mathrm{p}} = 0.05(R_{\mathrm{c}} = (1/4))$.

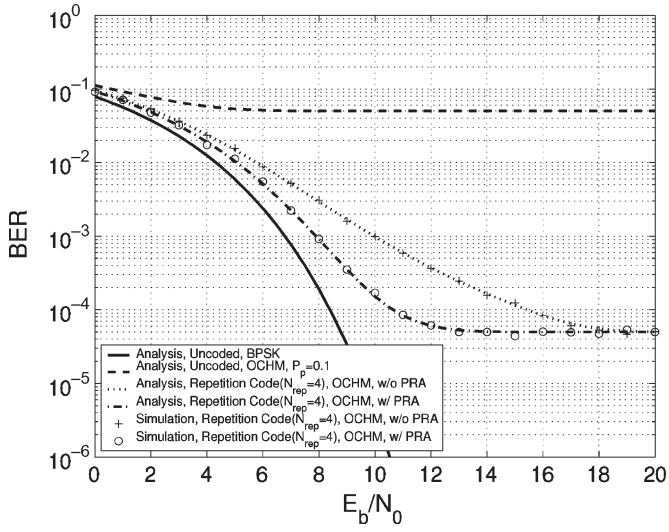

Fig. 5. Coded BER performance of RC with $P_{\mathrm{p}} = 0.1(R_{\mathrm{c}} = (1/4))$.

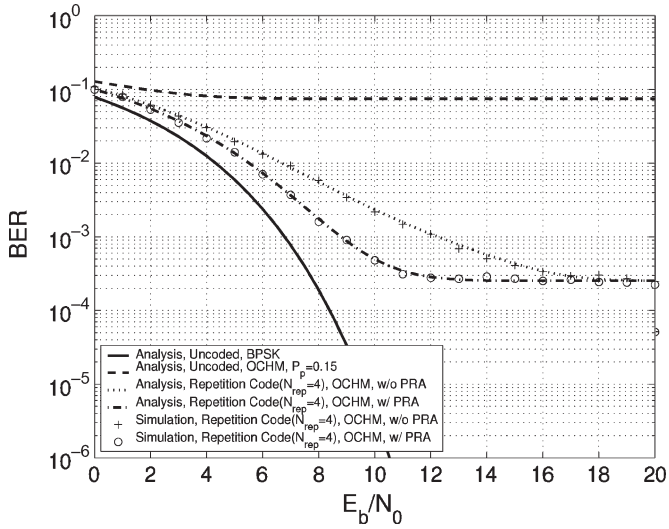

Fig. 6. Coded BER performance of RC with $P_{\mathrm{p}} = 0.15(R_{\mathrm{c}} = (1/4))$.

uncoded BER curves shown in (7) that vary the perforation probability (P_{p}), and the symbols without lines represent the computer simulation results. If the downlink total transmission power is smaller than the maximum transmission power, the mean channel activity of all downlink channels is 0.1, and the allowable perforation probabilities are set to 0.05, 0.10, and 0.15, then the number of allocatable downlink dedicated orthogonal channels with 64 OCs M is approximately 67, 136, and 209, respectively [3]. A channel activity of 0.1 is a reasonable assumption when we consider Internet data traffic such as Hypertext Transfer Protocol. The BER increases as the perforation probability increases. Moreover, as noted earlier, the uncoded BER is saturated by the perforation probability, and the saturated BER is given as $P_{\mathrm{p}}/2$. Therefore, in OCHM systems, the channel-coding capability is very important in satisfying a target BER or FER.

Figs. 4–6 show the BER performance of RCs, with/without power reallocation (PRA) in OCHM systems, for three different P_{p} values of 0.05, 0.1, and 0.15, respectively. We assume that the number of repetitions is four. In RC cases, regardless of the perforation probability, the simulation results agree very well with the analysis. As noted earlier, the RC has no coding gain in the conventional systems. Hence, in the conventional system, the BER performance of the RC is the same as that of the uncoded BPSK system, i.e., the solid lines in the figures. However, the RC can be an effective coding scheme in OCHM systems, since it reduces the saturated bit-error probabilities induced by perforations. Analysis results on the BER performance of the RC in the figures indicate (18) and (24). As the number of repetitions increases, the saturated bit-error probability decreases.

Furthermore, the proposed RC-PRA scheme improves the BER performance, compared with the conventional RC, even though it has the same saturated bit-error probability as a conventional RC. For example, the proposed RC-PRA scheme has a 4-dB energy gain, compared with the conventional RC for a BER value of 10^{-4} when the perforation probability is set to 0.1.

Fig. 7 shows the BER performance of the CCs with a constraint length (K) of three, i.e., the number of memories in

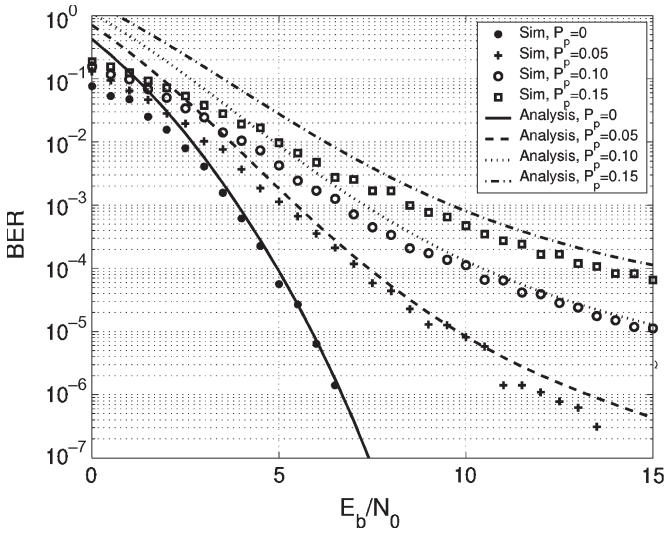

Fig. 7. BER performance of the CCs with $K = 3$ and $R_c = (1/2)$.

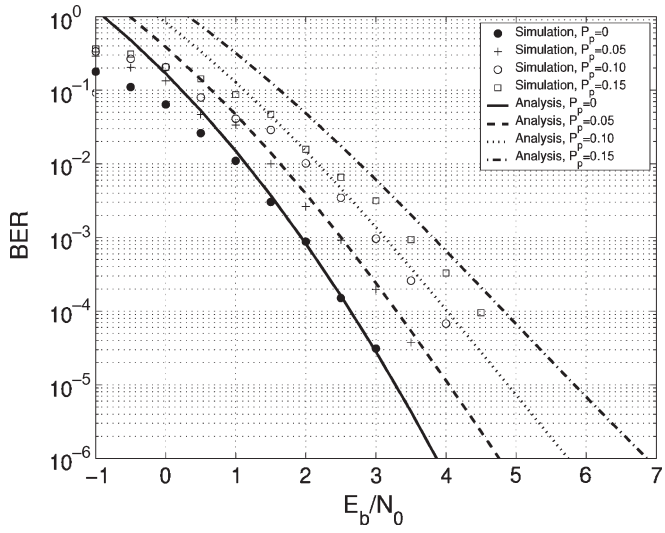

Fig. 8. BER performance of CC with $K = 9$ and $R_c = (1/3)$.

the encoder is two. The generator polynomial is (5, 7) in octal number, and the code rate is 1/2. Hence, the free distance (d_{free}) of the encoder is five, which dominates the coding performance. P_b is bounded as

$$P_b < \sum_{d=d_{\text{free}}}^{\infty} B_d P_d = 1 \cdot P_5 + 2 \cdot 2P_6 + 3 \cdot 4P_7 + \cdots + (k+1) \cdot 2^k P_{k+5} + \cdots \quad (47)$$

where P_d was given in (26) and (29) for the conventional systems and the OCHM systems, respectively. We plot the performance bounds and the simulation results as a function of E_b/N_0. The lines represent the bound in (28) in case that P_p is equal to zero, and they represent the bound in (31) in case that P_p is not equal to zero. The symbols without lines indicate the computer simulation results. Note that the bounds expressed in (28) and (31) agree very well with the simulation results for relatively high E_b/N_0 values. For lower E_b/N_0 values, however, the bounds deviate largely from the simulation results. The BER increases as the perforation probability P_p increases. When P_p is equal to 0.10, the additional required E_b/N_0 is 5 dB, compared with the conventional system for a 10^{-4} BER performance. If the channel-coding capability increases, the additional required E_b/N_0 decreases.

Fig. 8 shows another example of CCs. We also assume that BPSK is used as a modulation scheme and that the wireless channel is an AWGN channel. We utilize a CC of $R_c = 1/3$ and $K = 9$ with a generator polynomial (557, 663, 711) in octal number, and then, the free distance (d_{free}) of the encoder is 18. The CC was used in the IS-95 uplink system [14]. P_b is bounded as [20]

$$P_b < \sum_{d=d_{\text{free}}}^{\infty} B_d P_d = 11P_{18} + 32P_{20} + 195P_{22} + 564P_{24} + 1473P_{26} + 5129P_{28} + 17\,434P_{30} + 54\,092P_{32} + 171\,117P_{34} + \cdots \quad (48)$$

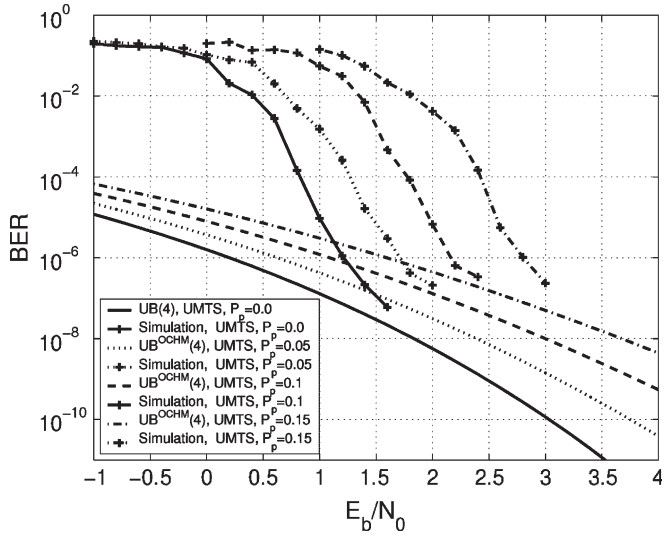

Fig. 9. BER performances of TC with $K = 4$ and $R_c = (1/3)$.

where B_d is obtained by a heuristic search in most cases. The bounds of (28) and (31) also agree with the simulation result in this case. The BER increases as the perforation probability increases. However, because of the enhanced coding performance, the additional required E_b/N_0 is significantly reduced, compared with the previous CC result shown in Fig. 7. When the P_p value is set to 0.10, the additional required E_b/N_0 is approximately 1.5 dB for 10^{-4} BER performance, which is significantly small, compared with that of the previous example. Therefore, in OCHM systems, the channel-coding performance is one of most important factors.

Fig. 9 shows the BER performance of the TC in OCHM systems. In this simulation, we use a TC used in the Universal Mobile Telecommunications System [1]. The code rate is 1/3, and the length of information block is 1024. We compute the free distance and coefficients of the first several terms in distance spectrum according to the Garello's algorithm, which is found in [21]. The lines without symbols indicate the result in (38) for OCHM and the result in (36) for $P_p = 0$. We

TABLE II
SATURATED BER AND FER OF VARIOUS CODING SCHEMES

Saturated BER				
P_p	RC (RC-PRA)	CC, K=3	CC, K=9	TC
0.05	3.13×10^{-6}	1.56×10^{-7}	2.1×10^{-23}	4.37×10^{-36}
0.10	5.00×10^{-5}	5.00×10^{-6}	5.5×10^{-18}	1.46×10^{-28}
0.15	2.53×10^{-4}	3.80×10^{-5}	8.1×10^{-15}	3.70×10^{-24}

Saturated FER				
P_p	RC (RC-PRA)	CC, K=3	CC, K=9	TC
0.05	3.2×10^{-3}	1.60×10^{-4}	2.15×10^{-20}	4.47×10^{-33}
0.10	5.12×10^{-2}	5.12×10^{-3}	5.63×10^{-15}	1.50×10^{-25}
0.15	2.59×10^{-1}	3.89×10^{-2}	8.29×10^{-12}	3.79×10^{-21}

TABLE III
REQUIRED E_b/I_0 AT MU ACCORDING TO $P_{\rm p}$ AND $\rm FER_{req}$

$FER_{req} = 10\%$ and $L_{frame} = 1024$					
P_p	RC	RC-PRA	CC, K=3	CC, K=9	TC
0.00	8.24 dB	8.24 dB	5.00 dB	2.63 dB	0.81 dB
0.05	11.21 dB	9.18 dB	7.23 dB	3.28 dB	1.28 dB
0.10	15.60 dB	10.52 dB	10.52 dB	4.02 dB	1.80 dB
0.15	∞	∞	15.51 dB	4.82 dB	2.41 dB

$FER_{req} = 1\%$ and $L_{frame} = 1024$					
P_p	RC	RC-PRA	CC, K=3	CC, K=9	TC
0.00	8.24 dB	8.24 dB	5.84 dB	3.30 dB	1.01 dB
0.05	15.61 dB	11.00 dB	9.78 dB	4.03 dB	1.46 dB
0.10	∞	∞	15.92 dB	4.89 dB	1.96 dB
0.15	∞	∞	∞	5.81 dB	2.55 dB

compute the first four terms in distance spectrum. Simulation results agree with the analytical ones for high E_b/N_0 values with a slight difference of about 0.5 dB, which is caused by the suboptimal iterative decoding used in the decoder. If the perforation probability is set to 0.15, the additional required E_b/N_0 at the receiver is about 1.5 dB for a BER value of 10^{-6}. If the required BER is lower than 10^{-6}, TC may be inefficient since it reaches the error-floor region and the slopes of BER performance decrease.

Table II summarizes the saturated BER and FER performance of three different types of coding schemes. The saturated FER is estimated for $L_{\rm frame} = 1024$. If the saturated FER of a coding scheme is larger than the required FER, the coding scheme cannot be used.

B. Additional Required Energy at MU

Table III summarizes the required E_b/I_0 of the three different types of coding schemes in Section V-A for the varying $\rm FER_{req}$ and $P_{\rm p}$ values, which is $f(\rm FER_{req}, P_{\rm p})$ as shown in Section IV-B. In Table III, RCs cannot be used in case that $\rm FER_{req} = 10\%$ and $P_{\rm p} = 0.15$, because they have larger saturated FER values than $\rm FER_{req}$. As noted earlier, the required E_b/N_0 increases as the $P_{\rm p}$ value increases, and BS should allocate more power to MUs with large $P_{\rm p}$ values, even though a coding scheme has smaller saturated FER values than $\rm FER_{req}$.

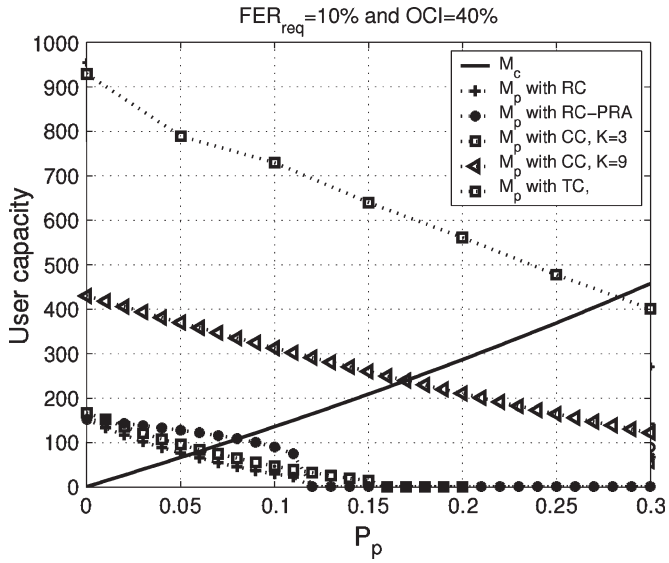

Fig. 10. User capacities of OCHM system with various channel coding schemes.

Allocation of more power to MUs limits the power capacity. Therefore, the coding scheme used for OCHM is a key factor affecting the performance of OCHM. If an MU requires larger power than a limit due to its perforations, a BS needs to perform an appropriate admission control scheme in order to save power consumption.

C. User Capacity With Various Coding Schemes

The OCHM system circumvents the code-limit situation by allowing HP collisions among active MUs. However, the HP collisions degrade the link-level performance. Thus, each MU requires more energy for the same FER performance as compared with that of the conventional systems. It decreases the power capacity. Since the overall capacity is the minimum value of the code and the power capacities, the additional required energy at MU for varying the $P_{\rm p}$ values is a most important factor in determining the capacity. Therefore, the channel-coding capability is very important in OCHM systems. As shown in (44), the code capacity of the OCHM system increases as $P_{\rm p}$ increases, while the power capacity of the OCHM system decreases as $P_{\rm p}$ increases, as shown in (46). Hence, the overall capacity is determined at the intersection of two capacities.

Fig. 10 shows $M_{\rm c}$ and $\tilde{M}_{\rm p}$ of the OCHM system for the three different channel coding schemes. The $\rm FER_{req}$ value is set to 0.1, and the other-cell interference (OCI) represents the loading factor of other cells, which is the ratio of the transmitted power to the maximum transmit power at the other cell BS. $N_{\rm OC}$ is equal to 64. The other parameters used to compute $\tilde{M}_{\rm p}$ in Fig. 10 are derived from [6]. We assume an omnidirectional antenna and a channel activity of 0.1. As noted before, $M_{\rm c}$ increases as $P_{\rm p}$ increases, while $\tilde{M}_{\rm p}$ decreases, and thus, the overall capacity of the OCHM system is determined at the intersection of both capacities. If we use a better channel coding scheme in the downlink, we can obtain improved user capacity. Note that $M_{\rm c}$ may vary according to HP-generation methods. In Fig. 10, we assume that the HP is randomly generated.

TABLE IV
INFORMATION DATA RATES OF VARIOUS CODING SCHEMES

$N_{OC}=64$, $W=3.84MHz$, $m=2$ $(BPSK)$					
	RC	RC-PRA	CC, K=3	CC, K=9	TC
R_c	$1/4$	$1/4$	$1/2$	$1/3$	$1/3$
R_{info}	$15Kbps$	$15Kbps$	$30Kbps$	$20Kbps$	$20Kbps$

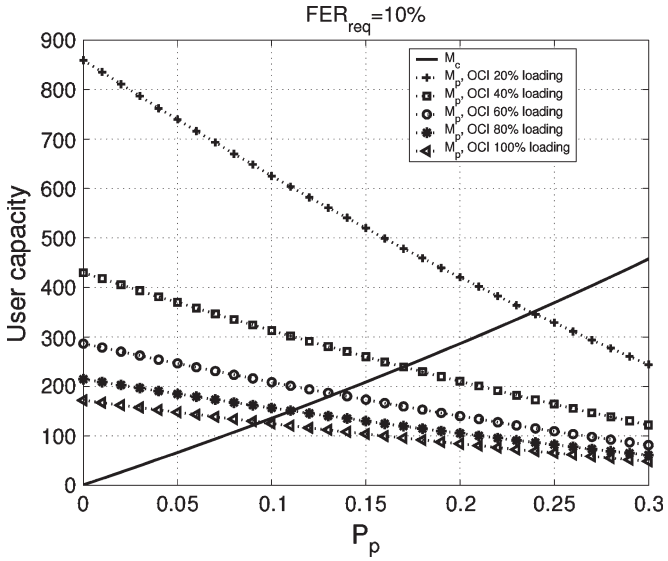

Fig. 11. User capacities of OCHM system for varying OCI of CC with $K=9$.

TABLE V
OVERALL USER CAPACITIES OF OCHM SYSTEMS WITH VARIOUS CODING SCHEMES

$FER_{req}=10\%$, $L_{frame}=1024$, $\bar{\nu}=0.1$, $N_{OC}=64$, $W=3.84MHz$, $m=2$ $(BPSK)$					
OCI	RC	RC-PRA	CC, K=3	CC, K=9	TC
20%	100	150	117	349	524
40%	72	109	83	240	363
60%	58	81	64	184	283
80%	47	64	53	151	231
100%	39	53	44	128	197

Furthermore, each channel coding scheme has a different code rate, and thus, the information rate (R_{info}) is also different.

Table IV shows the information data rates of OCHM systems for the three different coding schemes. We assume that the system bandwidth is 3.84 MHz, which is the same as that of the Third Generation Partnership Project Wideband CDMA (WCDMA) system.

Fig. 11 shows the user capacities for varying the OCI of a CC with $K=9$. As the OCI increases, user capacity decreases since $\tilde{M}_{\text{p}}$ decreases. User capacity is determined at the intersection of both code capacity and power capacity for given OCI environments. Table V summarizes the overall user capacities of OCHM systems for various coding schemes for the varying OCI values. If we utilize the TC at the BS as a channel coding scheme, more than 400 users can be accommodated in the downlink, which is much larger than the number of OCs $(N_{\text{OC}}=64)$.

VI. CONCLUSION

In this paper, we introduced a received-signal model: POM, in OCHM systems. A POM provides a lower bound of the BER performance in OCHM systems. The BER performance of OCHM systems is analyzed in both uncoded and various coded environments. The BER performance is saturated by the perforation probability in an uncoded environment. For the coded BER performance analysis, the RC, CC, and TC are compared. There also exist BER saturations in coded environments, even though they are highly reduced by coding techniques. We proposed an RC-PRA scheme in OCHM, which improves the BER performance and user capacity, compared with the conventional RC in OCHM sytems. The analytical results of various coded OCHM systems agree well with computer simulation results. Through analytical results, we can compute the additional required energy at the receiver to compensate for perforations and adjust the power level for a target BER performance at the receiver, according to given perforation probabilities. In addition, the user capacity of OCHM can be estimated for a given channel coding scheme, considering both code and power capacities.

REFERENCES

[1] *Physical Layer Aspects of ULTRA High Speed Downlink Packet Access (Release 4)*, Mar. 2001. 3GPP TR25.848 V4.0.0.
[2] *cdma2000 High Rate Packet Data Air Interface Specification*, Oct. 2000. 3GPP2. C.S0024 v.4.0.
[3] S. Park and D. K. Sung, "Orthogonal code hopping multiplexing," *IEEE Commun. Lett.*, vol. 6, no. 12, pp. 529–531, Dec. 2002.
[4] J. K. Kwon, S. Park, and D. K. Sung, "Log-likelihood conversion schemes in orthogonal code hopping multiplexing," *IEEE Commun. Lett.*, vol. 7, no. 3, pp. 104–106, Mar. 2003.
[5] J. H. Chung, S. Park, and D. K. Sung, "Symbol perforation reduction schemes for orthogonal code hopping multiplexing," *IEICE Trans. Commun.*, vol. E88-B, no. 10, pp. 4107–4111, Oct. 2005.
[6] S. H. Moon, S. Park, J. K. Kwon, and D. K. Sung, "Capacity improvement in CDMA downlink with orthogonal code hopping multiplexing," *IEEE Trans. Veh. Technol.*, vol. 55, no. 2, pp. 510–527, Mar. 2006.
[7] J. K. Kwon, S. Park, and D. K. Sung, "Collision mitigation by log-likelihood ratio (LLR) conversion in orthogonal code hopping multiplexing," *IEEE Trans. Veh. Technol.*, vol. 55, no. 2, pp. 709–717, Mar. 2006.
[8] E. A. Geraniotis and M. B. Pursley, "Error probability for slow-frequency-hopped spread-spectrum multiple-access communications over fading channels," *IEEE Trans. Commun.*, vol. COM-30, no. 5, pp. 996–1009, May 1982.
[9] B. C. Jung, J. H. Chung, and D. K. Sung, "Symbol repetition and power re-allocation scheme for orthogonal code hopping multiplexing systems," in *Proc. APCC/MDMC*, Aug. 2004, pp. 80–84.
[10] A. Papoulis and S. U. Pillai, *Probability, Random Variables, and Stochastic Processes*. New York: McGraw-Hill, 2002.
[11] J. G. Proakis, *Digital Communications*. New York: McGraw-Hill, 1995.
[12] A. J. Viterbi, "Convolutional codes and their performance in communication systems," *IEEE Trans. Commun.*, vol. COM-19, no. 5, pp. 751–772, Oct. 1971.
[13] S. Lin and D. J. Costello, *Error Control Coding*. Englewood Cliffs, NJ: Prentice-Hall, 2004.
[14] J. S. Lee and L. E. Miller, *CDMA Systems Engineering Handbook*. Norwood, MA: Artech House, 1998.
[15] C. Berrou, A. Glavieux, and P. Thitimajshima, "Near Shannon limit error-correcting coding an decoding: Turbo codes," in *Proc. IEEE ICC*, May 1993, pp. 1064–1070.
[16] S. Benedetto and G. Montorsi, "Unveiling turbo codes: Some results on parallel concatenated coding," *IEEE Trans. Inf. Theory*, vol. 42, no. 2, pp. 409–428, Mar. 1996.
[17] S. Benedetto and G. Montorsi, "Design of parallel concatenated convolutional codes," *IEEE Trans. Commun.*, vol. 44, no. 5, pp. 591–600, May 1996.

[18] L. C. Perez, J. Seghers, and D. J. Costello, Jr., "A distance spectrum interpretation of turbo codes," *IEEE Trans. Inf. Theory*, vol. 42, no. 6, pp. 1698–1709, Nov. 1996.
[19] R. Garello, P. Pierleoni, and S. Benedetto, "Computing the free distance of turbo codes and serially concatenated codes with interleavers: Algorithms and applications," *IEEE J. Sel. Areas Commun.*, vol. 19, no. 5, pp. 800–812, May 2001.
[20] J. Conan, "The weight spectra of some short low-rate convolutional codes," *IEEE Trans. Commun.*, vol. COM-32, no. 9, pp. 1050–1053, Sep. 1984.
[21] [Online]. Available: http://www.tlc.polito.it/garello/turbodistance/turbodistance.html

Bang Chul Jung (S'02) received the B.S. degree in electronics engineering from Ajou University, Suwon, Korea, in 2002 and the M.S. degree in electrical engineering from Korea Advanced Institute of Science and Technology (KAIST), Daejeon, Korea, in 2004, where he is currently working toward the Ph.D. degree.

Since 2004, he has also been a Teaching and Research Assistant with the Department of Electrical Engineering and Computer Science, KAIST. His research interests include orthogonal-code hopping systems for packet-data transmission, orthogonal frequency-division multiplexing systems, radio-resource management, wireless-scheduling algorithms, information theory, link- and system-level simulations for 3G and 4G wireless communication systems, adaptive modulation and coding, and multiple-input–multiple-output systems.

Dan Keun Sung (S'82–M'85–SM'00) received the B.S. degree in electronics engineering from Seoul National University, Seoul, Korea, in 1975 and the M.S. and Ph.D. degrees in electrical and computer engineering from the University of Texas at Austin, in 1982 and 1986, respectively.

From May 1977 to July 1980, he was a Research Engineer with the Electronics and Telecommunications Research Institute, where he was engaged in various projects, including the development of an electronic switching system. In 1986, he joined the faculty of Korea Advanced Institute of Science and Technology (KAIST), Daejeon, Korea, where he is currently a Professor with the Department of Electrical Engineering and Computer Science. From 1996 to 1999, he was a Director with the Satellite Technology Research Center, KAIST. His research interests include mobile communication systems and networks, high-speed networks, next-generation IP-based networks, traffic control in wireless and wireline networks, signaling networks, intelligent networks, performance and reliability of communication systems, and microsatellites.

Dr. Sung is an Editor of the *IEEE Communication Magazine*. He was a Division Editor of the *Journal of Communications and Networks*. He was a Vice Chair of the ICC 2002 Symposium on Global Service Portability and Infrastructure for Next Generation Virtual Home and Office Environments and a Program Cochair of the Globecom 2002 Symposium on Service Infrastructure for Virtual Enterprise Environments. He was also the General Conference Chair and the Technical Program Committee Vice Chair of ICC 2005. He was the recipient of the National Order of Merits, the Dongbaek Medal in 1992, the Research Achievement Award in 1997, the MoMuc Paper Award in 1997, the Academic Excellence Award in 2000, the Best Paper Award at APCC2000, and This Month's Scientist Award from MOST and KOSEF in 2004. He is a member of the Institute of Electronics, Information, and Communication Engineers and Korea Information and Communications Society. He is also a member of Phi Kappa Phi and Tau Beta Pi.